Nonlinearity Domination in Hassellmann Equation as a Reason for Alternative Framework of its Numerical Simulation

Vladimir Zakharov, Andrei Pushkarev
Waves and Solitons LLC
1719 W. Marlette Ave.
Phoenix, AZ 85015
phone: +1 (602) 748-4286 e-mail: dr.push@gmail.com

Award Number: N00014-10-1-0991

LONG TERM GOALS

Development of accurate and fast advanced statistical and dynamical nonlinear models of ocean surface waves, based on first physical principles, which will improve and accelerate both long term ocean surface wave turbulence forecasts and prediction of strongly coherent events, such as freak waves and wave-breakings.

OBJECTIVES

Creation of better statistical models for improvement of existing operational wave prediction programs; study of non-stationary waves growth in presence of wind; interpretation of experimental data through study of self-similar solutions of Hasselmann equation; studying the integrability of 1D dynamical equations for surface waves; study of the possibility of generalization of compact 1D water waves equation for 2D situation; study of the implications of modulational instability on solitons, rogue waves and air-surface interaction.

APPROACH

Numerical methods for solution of integro-differential equations; analytical self-similar solutions for integro-differential equations; Hamiltonian formalism; comparison of analytical and numerical solutions with experimental data; analytical and numerical solution of approximate models for deep water surface waves

WORK COMPLETED

- We propose to use new wind forcing source term, which is analytical solution of Hasselmann equation, consistent with experimental data and numerical simulation
- We prove that there is no reason to include dissipation in the spectral maximum area. Instead, we justify localization of dissipation in high wave-numbers area
- We re-examine energy balance in the wind-driven sea and find that the major term in the energy balance is nonlinear interaction term S_{nl}. This fact explains Kolmogorov-Zakharov

Report Documentation Page

Form Approved
OMB No. 0704-0188

1. REPORT DATE	2. REPORT TYPE	3. DATES COVERED
30 SEP 2014		**00-00-2014 to 00-00-2014**

4. TITLE AND SUBTITLE	5a. CONTRACT NUMBER
Nonlinearity Domination in Hassellmann Equation as a Reason for Alternative Framework of its Numerical Simulation	5b. GRANT NUMBER
	5c. PROGRAM ELEMENT NUMBER
6. AUTHOR(S)	5d. PROJECT NUMBER
	5e. TASK NUMBER
	5f. WORK UNIT NUMBER
7. PERFORMING ORGANIZATION NAME(S) AND ADDRESS(ES) **Waves and Solitons LLC,1719 W. Marlette Ave,Phoenix,AZ,85015**	8. PERFORMING ORGANIZATION REPORT NUMBER
9. SPONSORING/MONITORING AGENCY NAME(S) AND ADDRESS(ES)	10. SPONSOR/MONITOR'S ACRONYM(S)
	11. SPONSOR/MONITOR'S REPORT NUMBER(S)

12. DISTRIBUTION/AVAILABILITY STATEMENT
Approved for public release; distribution unlimited

13. SUPPLEMENTARY NOTES

14. ABSTRACT

15. SUBJECT TERMS

16. SECURITY CLASSIFICATION OF:			17. LIMITATION OF ABSTRACT	18. NUMBER OF PAGES	19a. NAME OF RESPONSIBLE PERSON
a. REPORT **unclassified**	b. ABSTRACT **unclassified**	c. THIS PAGE **unclassified**	**Same as Report (SAR)**	**27**	

weak-turbulent spectra $I_\omega \sim \omega^{-4}$ and $I_\omega \sim \omega^{-11/3}$ and self-similar behavior both in experimental observations and numerical simulation as well

- We propose new framework for simulation of Hasselmann equation based on exact nonlinear interaction term in Webb-Resio-Tracy (***WRT)*** form, new wind input term and wave-breaking damping localized in high wave-numbers
- We found that majority of field and wave tank experimental data can be explained in terms of self-similar solution of the Hasselmann kinetic equation. The self-similarity explains persistence of the "magic links" connecting indices of energy and mean frequency dependencies in fetch- and duration-limited setups
- We analyzed proposed alternative framework for HE simulation through massive numerical experiments of Hasselmann equation and found that they reproduce more than a dozen of field experiments
- Based on the idea of nonlinearity domination and self-similarity, we developed the set of tests allowing separating physically based wind input terms from non-physical ones
- We show that central role of self-similar regimes explains very simple "universality of the wind-driven sea", connecting average steepness, frequency of the spectral peak and fetch. This universality is observed in majority of field and wave tank experiments. This is strong confirmation of our basic concepts
- We propose and compare with the original exact 1D Euler dynamical equation its cost-effective simplification
- We analyze relation of modulational instability and coherent events such as solitons and freak waves
- We study the peculiarities of breaking waves and air flow interaction, allowing to understand air structures formation and their influence on surface waves

RESULTS

1. **Alternative framework for Hasselmann equation simulation**

It is generally accepted nowadays that ocean surface wave turbulence is described by Hasselmann equation (HE)

$$\frac{\partial \varepsilon}{\partial t} + \frac{\partial \omega_k}{\partial \vec{k}} \frac{\partial \varepsilon}{\partial \vec{r}} = S_{nl} + S_{in} + S_{diss}$$

for spectral energy density $\varepsilon = \varepsilon(\vec{k}, \vec{r}, t)$, wave dispersion $\omega = \omega(k)$ and nonlinear, wind input and wave-breaking dissipation terms S_{nl}, S_{in} and S_{diss} correspondingly.

While this acceptance implicitly assumes that HE is some sort of mathematical reduction of primordial Euler equations for incompressible fluid with free surface, it is true, in fact, only for advection $\frac{\partial \omega_k}{\partial \vec{k}} \frac{\partial \varepsilon}{\partial \vec{r}}$ and four-wave interaction S_{nl} terms.

As far as concerns S_{in} and S_{diss} terms, there is no consensus in the worldwide oceanographic community about their parameterization. To our belief, it is the one of the reasons, indeed, for "tuning knobs" (adjusting coefficients) necessity in operational models for their adjustment to changing ocean situations.

Another reason for using "tuning knobs" is underestimation of the leading role of S_{nl}. In other words, the role of the "tuning knobs" also consists in "undoing" the deformation incurred to the model through substituting of the exact S_{nl} nonlinear term with DIA-like simplifications.

Current state of S_{in} wind input source terms

Nowadays, the number of existing models of S_{in} is large, but neither of them have firm theoretical justification. Different theoretical approaches argue with each other. A detailed description of this discussion can be found in paper **[R1]** and monograph **[R2]**. Other models are presented in papers **[R3]-[R7]**. The majority of S_{in} models follow quasi-linear Miles approach **[R8]**. While we believe that this approach is the most relevant, the self-consistent derivation of S_{in} in the framework of this approach is hampered by the lack of information about fine structure of turbulent atmospheric boundary layer near the sea surface.

A systematic experimental study of this structure has just been started (see, for instance, the remarkable article **[R9]**). Experimental data about S_{in} are scarce. Moreover, in some cases experiments interpretation could be seriously criticized.

Let's get to the point in the details.

Consider the so-called "method of fractional growth" **[R10]**, **[R11]** and **[R3]**. The first starting equation in those publications (up to the constants) is:

$$\gamma = \frac{1}{\varepsilon(\omega)} \frac{\partial \varepsilon(\omega)}{\partial t} \tag{1}$$

which is, in fact, the linear part, or just two terms of the energy balance HE:

$$\frac{\partial \varepsilon}{\partial t} + \frac{\partial \omega_k}{\partial \vec{k}} \frac{\partial \varepsilon}{\partial \vec{r}} = S_{nl} + \gamma \varepsilon \tag{2}$$

In this approach advection $\frac{\partial \omega_k}{\partial \vec{k}} \frac{\partial \varepsilon}{\partial \vec{r}}$ and nonlinear S_{nl} terms of HE are absent. Why are those terms neglected? Why, if this absence is justified, so many efforts were spent to improve the numerical simulation of nonlinear term S_{nl}? Wouldn't it be easier just to solve analytically the linear Eq. (1)? Perhaps, some members of oceanographic community believe that equalization of the $\frac{\partial \varepsilon}{\partial t}$ and $\gamma \varepsilon$ terms in the balance equation (2) could be justified by the fact that the leading term in the equation is defined by conservative (in a sense of wave action, not energy and momentum) relationship

$$\frac{\partial \omega}{\partial \vec{k}} \frac{\partial \varepsilon}{\partial \vec{r}} = S_{nl}$$

Such equalization of two small terms in presence of two big ones is a not a good practice, in our opinion.

In a sense, the above author's stance is understandable, since the measurements of neither advection $\frac{\partial \omega_k}{\partial \vec{k}} \frac{\partial \varepsilon}{\partial \vec{r}}$, nor nonlinear S_{nl} terms are easy. But inability of measurement of those important terms cannot be acquittal for using wrong equations. Moreover, even if they managed to measure somehow advection $\frac{\partial \omega_k}{\partial \vec{k}} \frac{\partial \varepsilon}{\partial \vec{r}}$ and S_{nl} terms, how would they separate the effects of the wind forcing and the dissipation in γ?

In fact, the same trick was also used by W. J. Plant in his well-know paper in 1982 **[R15]**, but Plant emphasized that Eq.(1) can be used only *"...**if the wind speed is suddenly increased from zero...**"* (see p.162, upper left column). Such situations can be realized in a wave tank at the very beginning of waves excitation by the wind, but can not be applied for the situation of limited fetch (which is almost always present in the measurements) growth experiments and/or developed seas.

In a nutshell, such measurements use inappropriate interpretation technique, and the conclusions based on them cannot be considered as trustworthy ones.

To stress the level of scatter in different models of S_{in}, we refer to fundamental review article **[R16]** "Wave modeling -- the state of art", published in *"Progress of Oceanography"* in 2007 by members of *WISE* group. In this paper a reader can find two different expressions for dimensionless quantity

$$\gamma = \frac{\rho_a}{\rho_w} \omega \, q \left(\frac{\omega}{\omega_0} \right)$$

where $\omega_0 = \frac{g}{u_{10}}$, the Eqs. (2.2) and (2.4) of the manuscript. For the case $\omega = 3\omega_0$, Eq. (2.2) gives $q = 0.40$, while Eq.(2.4) gives $q = 1.23$ -- the difference of three times! Notice that the equation for our new wind input term

$$q = 0.05 \left(\frac{\omega}{\omega_0} \right)^{4/3}$$

gives $q = 0.216$.

In reality, nonlinear S_{nl} term is the ***leading*** term in ocean energy balance **[R12], [R13]**. It consists of two parts:

$$S_{nl} = F_k - \Gamma_k \varepsilon_k$$

which almost compensate each other. Otherwise, one cannot explain persistent presence of Zakharov - Filonenko asymptotic $I_\omega \sim \omega^{-4}$ which is the exact solution of the equation $S_{nl} = 0$. Such asymptotic of the rear face of the spectrum is observed in almost all field setups (including experiments by Resio and Long **[R20]**, **[R21]**) and many numerical calculations (for instance **[R17], [R18]**).

It was numerically shown in papers **[R12]**, **[R13]** that in typical situation $\Gamma_k \varepsilon_k$ surpasses S_{in} by the order of magnitude. Together with ubiquity of ω^{-4} asymptotic this is the clear manifestation of S_{nl} domination. Notice that this statement was actually formulated by K. Hasselmann and collaborators in 1976 **[R14]**.

It is important, therefore, to consider S_{in} wind input term as a perturbation to leading S_{nl} nonlinear term. For fetch limited case this approach was realized in our work **[R19]** through finding specific self-similar solution of HE

$$\varepsilon = t^{p+q} F(\omega t^q) \tag{3}$$

$$10q - 2p = 1 \tag{4}$$

Assumption that the new wind input term has the form

$$S_{in} = \gamma\varepsilon \sim \omega^{s+1}$$

and comparison with the results of experimental observations **[R20]**, **[R21]** allows finding corresponding exponents

$$s = \frac{4}{3}, \quad \mathrm{q} = \frac{3}{10}, \quad p = 1 \tag{5}$$

Those dependencies lead to the dependencies of total energy

$$\varepsilon = \varepsilon_0 x^p \tag{6}$$

and frequency

$$\omega = \omega_0 x^{-q} \tag{7}$$

on the fetch coordinate $\boldsymbol{x}$.

As a result, the new wind input term (named hereafter ***ZRP*** forcing) takes the form

$$S_{in} = \gamma\varepsilon, \quad \gamma = 0.05 \frac{\rho_{air}}{\rho_{water}} \omega \left(\frac{\omega}{\omega_0} \right)^{4/3} f(\theta) \tag{8}$$

$$f(\theta) = \begin{cases} \cos^2 \theta \ \text{ for } -\pi/2 \le \theta \le \pi/2 \\ 0 \ \text{ otherwise} \end{cases}$$

$$\omega_0 = \frac{g}{u_{10}}, \quad \frac{\rho_{air}}{\rho_{water}} = 1.3 \cdot 10^{-3}$$

The coefficient ***0.05*** in front of the new wind input term Eqs.(8) was found through carefully performed numerical experiments (which used ***exact*** **WRT** form of S_{nl} term**)** via tuning the S_{in} term to maximum number of experimental data.

Two scenarios of wave-breaking dissipation term S_{diss} : spectral peak or high-frequency domination?

In current section we explain why there is no need to use dissipation in the spectral peak area.

The spectral peak frequency damping is widely accepted practice, and is included as an option in the operational models ***WAM, SWAN*** and ***WAVEWATCH***. Historically, it was apparently done by need.

Consider, for example, Snyder's version of S_{in}, which is no better justified then others, but for no clear reason is more popular. We tested Snyder's version of S_{in} in our model and found that it is too strong (will be shown below), since it leads to the wave energy levels exceeding experimentally observable by several times. Obviously, to get acceptable energy levels, one had to add extra low-frequency damping, and that was apparently the reason for including damping in the spectral peak area.

Now let us proceed with the discussion of high-frequency dissipation function as possibly the most correct choice. Traditionally, it is usually argued that experimental observations **[R3]**, **[R4]** confirm that wave breaking of dominant waves is associated with energy loss near spectral peak. Here we explain why the energy loss in spectral peak vicinity ***does not necessary mean*** that damping is present in the spectral peak vicinity.

Wave-breaking is one-dimensional event in real space. First notice that analytical theory of such events is not developed yet. In out opinion, this theory can be based on the following fact: primordial Euler equations for potential flow of deep fluid with free surface has the self-similar solution

$$\eta(x,t) = gt^2 F\left(\frac{x}{gt^2}\right)$$

This solution was studied numerically in the framework of simplified ***MMT*** (Maida-MacLaughlin-Tabak) model of Euler equations **[R23]**.

In Fourier space this solution describes the propagation to high wave-numbers and returning back to dominant wave spectral peak of fat spectral energy tail, corresponding in real space to sharp wedge formation at $t = 0$ and space point $x = 0$. This solution describes formation of the "breaker".

In the absence of dissipation, this event is invertible in time. Presence of high-frequency dissipation chops off the end of the tail, just like “cigar cutter", and violates the tail’s invertability. Low and high harmonics, however, are strongly coupled in this event due to strong nonlinear non-local interaction, and deformed high wave-numbers tail is almost immediately returns to the area of spectral peak. As soon as fat spectral tail return to the area of the spectral peak, total energy in the spectrum diminishes, which causes settling of the spectral peak at lower level of energy. This process of "shooting" of the

spectral tail toward high wave-numbers, and its returning back due to wave breaking is the real reason of "sagging down" of the energy profile in the spectral peak area, but was erroneously associated with the presence of the damping in the area of spectral peak.

This explanation shows that individual wave-breakings studies **[R3], [R4]** are not the proof of spectral peak damping presence.

Also there is another, direct proof of the fact that damping is localized in the area of short waves. It is the measurements of quazi-one-dimensional "breakers" speed propagation -- strips of foam, which accompany any developed wave turbulence. Those airplane experiments, recently performed by P.Hwang and his team **[R24]**, **[R25]**, show that wave breakers propagate 4-5 times slower than crests of leading waves!

Based on the above discussion, we propose to use ***only high-frequency damping*** as a basis of alternative framework of HE simulation. One can "implicitly" insert this damping very easily without knowing its analytic form via spectral tail continuation by Phillips law $\sim \omega^{-5}$.

Replacement of high-frequency spectrum part by Phillips law is not our invention. It is the standard tool offered as an option in operational wave forecasting models, known as the "parametric tail", and corresponds to high-frequency dissipation, indeed. For the practical definition of Phillips tail it's necessary to know two more parameters: coefficient in front of it and starting frequency. The coefficient in front of ω^{-5} is unknown, but is unnecessary to be known in the explicit form – it is dynamically defined from the continuity condition of the spectrum. As far as concerns another unknown parameter – the frequency where Phillips spectrum starts – we define it as $f_0 = \frac{\omega_0}{2\pi} = 1.1\ Hz$ as per Resio and Long experimental observations **[R20], [R21]**. That is the way the high frequency ***implicit*** damping is incorporated into alternative computational framework of HE.

We think that the question of finer details of high-frequency damping structure is of secondary importance at current stage of alternative framework development.

Checking of the new modeling framework against theoretical predictions and experimental results

To check alternative framework for HE simulation, we performed numerical tests for waves excitation in limited fetch conditions using alternative framework. As it was already mentioned, alternative framework is based on exact nonlinear term S_{nl} in ***WRT*** form and ***ZRP*** new wind input term S_{in} in the form of Eqs.(8) **[R19]**.

Fig.1 shows that total energy is growing along the fetch by power law in accordance with Eq.(6) with ***p=1.0***

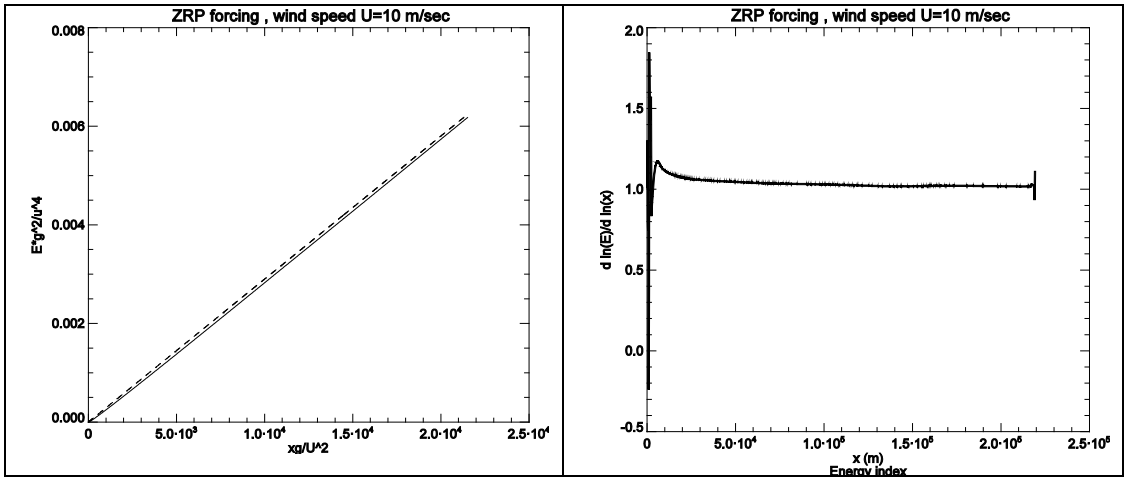

Fig.1 Left figure: solid line – numerical experiment, dashed line – fit by $2.9 \cdot 10^{-7} \cdot \frac{xg}{U^2}$.

Right figure: exponent p of the energy growth as the function of fetch x

Dependence of mean frequency of the fetch shown on ***Fig.2*** also demonstrates perfect correspondence of numerical results and corresponding self-similar solution dependence Eq.(7) with ***q=0.3***

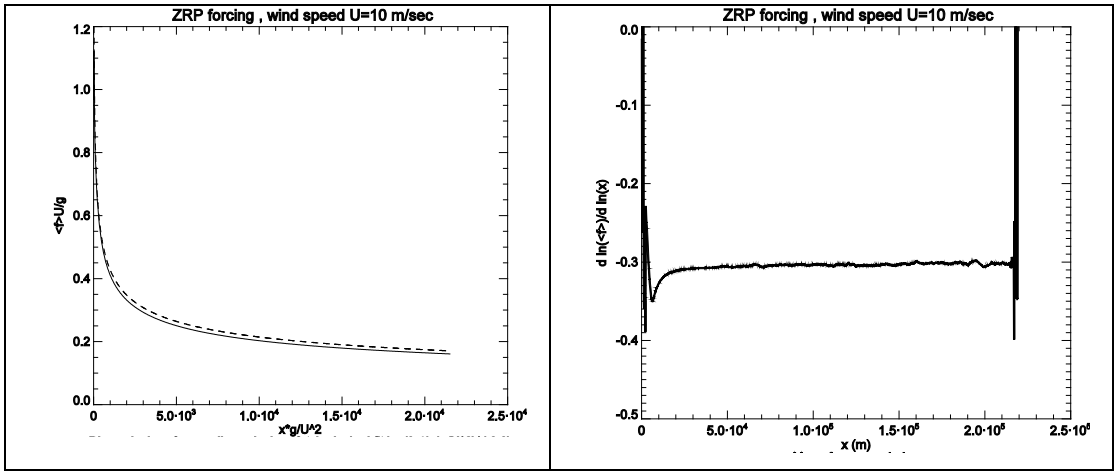

Fig.2 Left figure: solid line – numerical experiment, dashed line – fit by $3.4 \cdot \left(\frac{xg}{U^2}\right)^{-0.3}$.

Right figure: exponent of the energy growth as the function of fetch x

Left side of ***Fig.3*** presents directional spectrum as a function of frequency in logarithmic coordinates. One can see that energy curve on the left figure consists of segments of:

- the spectral maximum area
- Kolmogorov-Zakharov spectrum $\sim \omega^{-4}$
- Phillips high frequency tail $\sim \omega^{-5}$

Right side of ***Fig.3*** shows log-log derivative of the spectral curve from the left figure, which corresponds to the exponent of the local power law. Again, one can see the areas corresponding to Kolmogorov-Zakharov index ***-4*** and Phillips index ***-5***. The value of the index to the left side from ***-4***

has the tendency to grow, which qualitatively corresponds to the "inverse cascade" Kolmogorov-Zakharov index ***-11/3***.

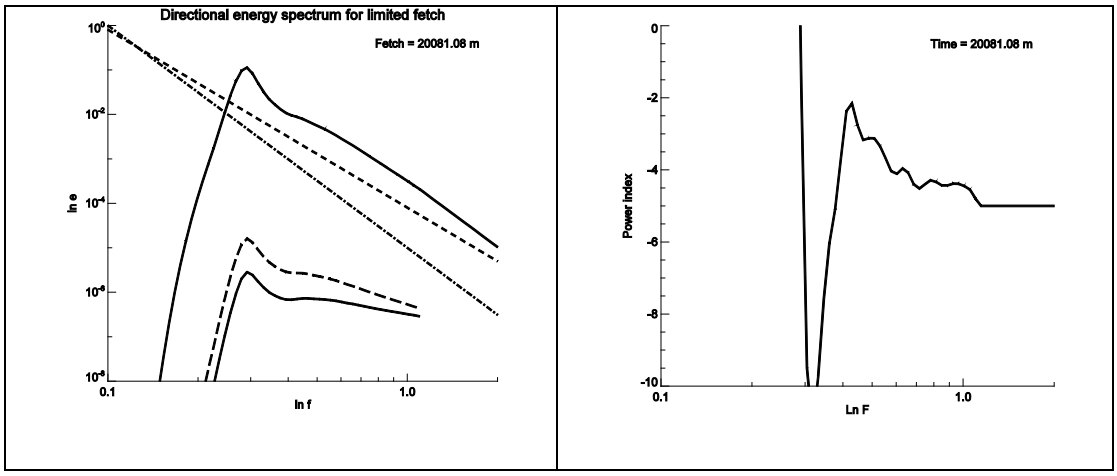

Fig.3 Left figure: upper solid line – logarithm of spectral density as a function of logarithm of frequency $f = \dfrac{\omega}{2\pi}$***, dashed line – fit*** $\sim \omega^{-4}$***, dash-dotted line – fit*** $\sim \omega^{-5}$***. Right figure: local exponent of*** ω ***calculated from the left figure***

Fig.4 present combination ***(10q-2p)*** as function of fetch ***x***. It is in perfect accordance with self-similar prediction Eq.(4).

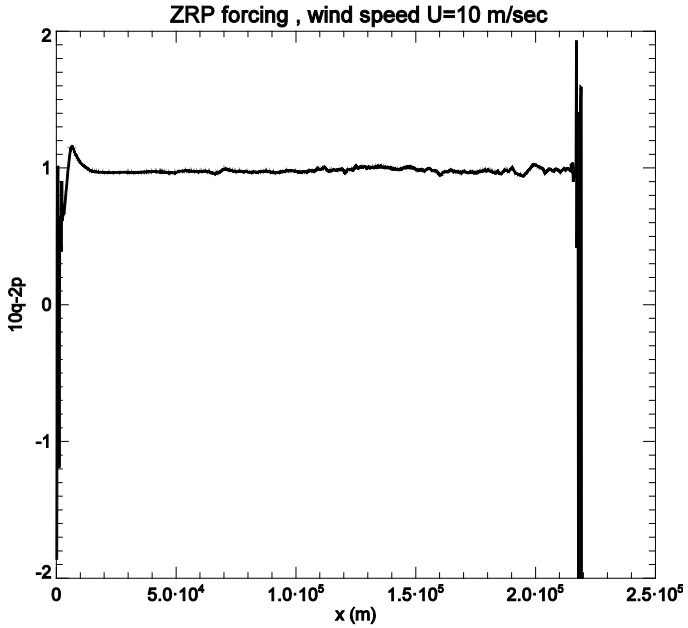

Fig.4 "Magic relation" (10q-2p) as a function of the fetch x

We conclude that alternative framework of HE simulation reproduces the following analytical features of HE:

- Self-similar solutions with correct exponents
- Kolmogorov-Zakharov spectra $\sim \omega^{-4}$

Table 1 presents results of calculation of exponents p and q (see Eqs.(3)-(7)) for 14 different experimental observations. The last row presents them for above described ZRP numerical experiment for limited fetch growth within alternative framework. One can see good correspondence between the theoretical, experimental and numerical values of p and q.

Experiment	***p***	***q***
Black Sea (Babanin & Soloviev 1998b)	0.89	0.275
Walsh et al. (1989) US coast	1.0	0.29
Kahma & Calkoen (1992) unstable	0.94	0.28
Kahma & Pettersson (1994)	0.93	0.28
JONSWAP by Davidan (1980)	1.0	0.28
JONSWAP by Phillips (1977)	1.0	0.25
Kahma & Calkoen (1992) composite	0.9	0.27
Kahma (1981, 1986) rapid growth	1.0	0.33
Kahma (1986) average growth	1.0	0.33
Donelan *et al.* (1992) St Claire	1.0	0.33
Ross (1978), Atlantic, stable	1.1	0.27
Liu & Ross (1980), Michigan, unstable	1.1	0.27
JONSWAP (Hasselmann *et al.* 1973)	1.0	0.33
Mitsuyasu *et al.* (1971)	1.008	0.33
ZRP numerics	**1.0**	**0.3**

Table 1

Tests for separation of trustworthy wind input terms S_{in} from non-physical ones.

As it was already discussed, nowadays there are plenty of historically developed wind input terms. Analysis of nonlinear properties of HE in the form of specific self-similar solutions and Kolmogorov-Zakharov law for direct energy cascade allows us to propose set of test, which would allow separation of physically justified wind-input terms S_{in} from non-physical ones.

As such, we propose:

- checking powers of observed energy and mean frequency dependencies along the fetch versus predicted by self-similar solutions
- checking the "magic relations" Eq.(4) between exponents ***p*** and ***q*** of observed energy and frequency dependencies along the fetch
- checking exponents of directional spectral energy dependencies versus Kolmogorov-Zakharov exponent ***-4***

We applied such tests to several popular wind input terms in fetch limited statement within alternative framework:

- Chalikov S_{in} term (see **[R26])**
- Snyder S_{in} term (see **[R27])**
- WAM3 S_{in} term (see **[R28])**

Test of Chalikov form of S_{in}

Fig.5 shows that total energy growth along the fetch significantly exceeds observed in ***ZRP*** simulation, and doesn't have correct value of exponent ***p=1.0***

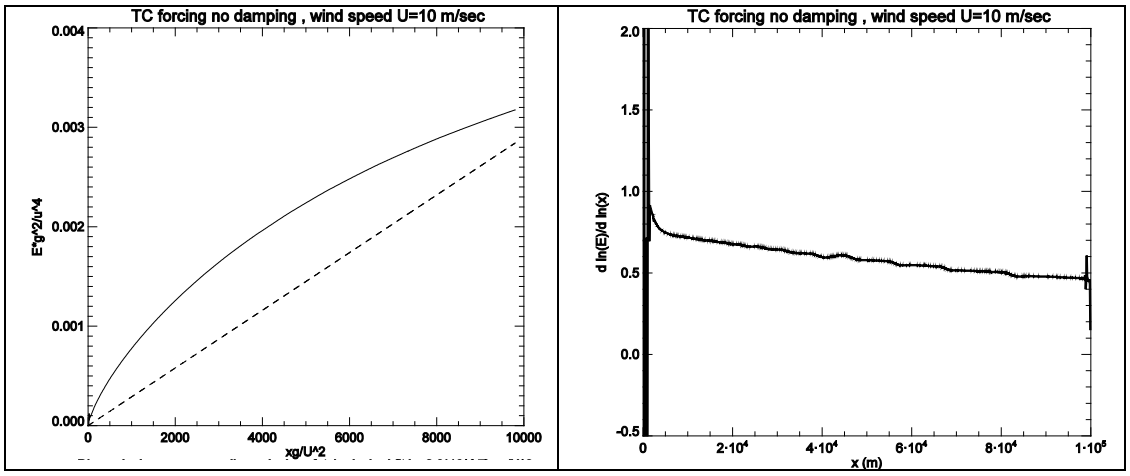

Fig.5 Same as Fig.1, but for Chalikov S_{in}

Dependence of mean frequency against the fetch shown on Fig.5 is also in poor correspondence with ***ZRP*** numerical results and corresponding self-similar exponent ***q=0.3***

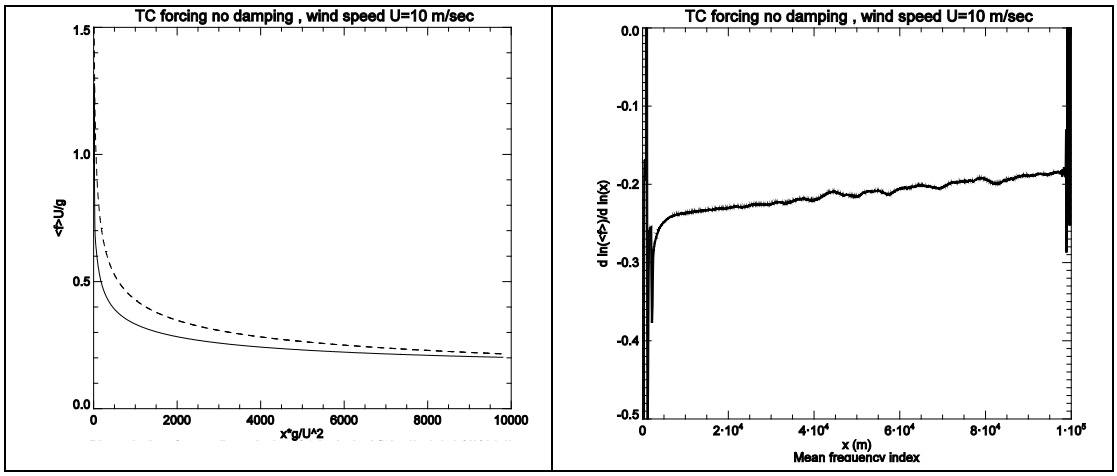

Fig.6 Same as Fig.2, but for Chalikov S_{in}

Left side of ***Fig.7*** presents directional spectrum as a function of frequency in logarithmic coordinates. One can see that similar to ***ZRP*** case we observe:

- the spectral maximum area

- Kolmogorov-Zakharov segment $\sim \omega^{-4}$
- Phillips high frequency tail $\sim \omega^{-5}$

Right side of ***Fig.7*** shows log-log derivative of the energy curve from ***Fig.5***, which corresponds to the exponent of the local power law. Again, one can see the areas corresponding Kolmogorov-Zakharov index ***-4*** and Phillips index ***-5***. The value of the index to the left side of ***-4*** has a tendency to grow, which qualitatively corresponds to the "inverse cascade" Kolmogorov-Zakharov index ***-11/3***.

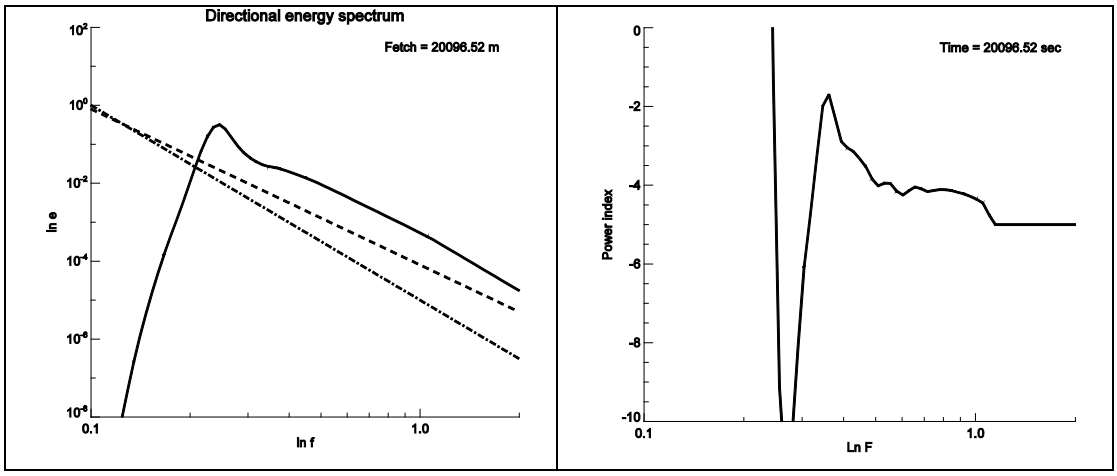

Fig.7 Same as Fig.3, but for Chalikov S_{in}

Fig.8 present combination ***(10q-2p)*** as a function of fetch distance ***x***. It is surprising that it is in perfect accordance with the relation Eq.(4) ! It mean that despite incorrect values ***p*** and ***q*** along the fetch, their combination ***(10q-2p)*** still holds in complete accordance with theoretical prediction, i.e. self-similarity is fulfilled ***locally.***

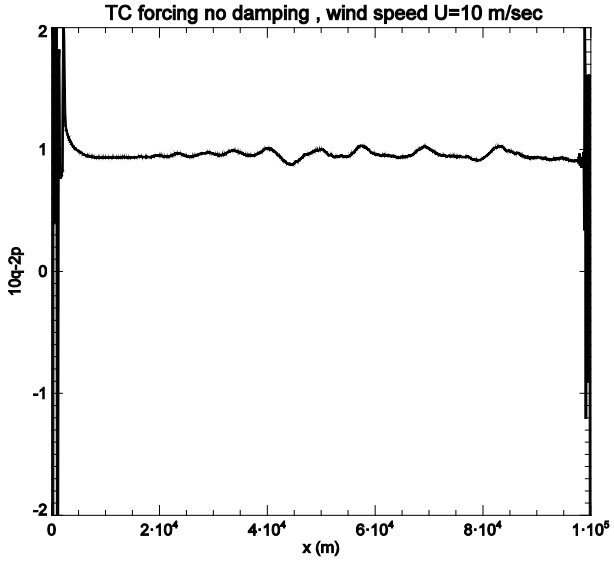

Fig.8 Same as Fig.4, but for Chalikov S_{in}

Test of Snyder form of S_{in}

Fig.9 shows that total energy growth along the fetch significantly exceeds ***ZRP*** simulation, but has the value of growth exponent close to ***p=1.0*** versus fetch coordinate ***x***.

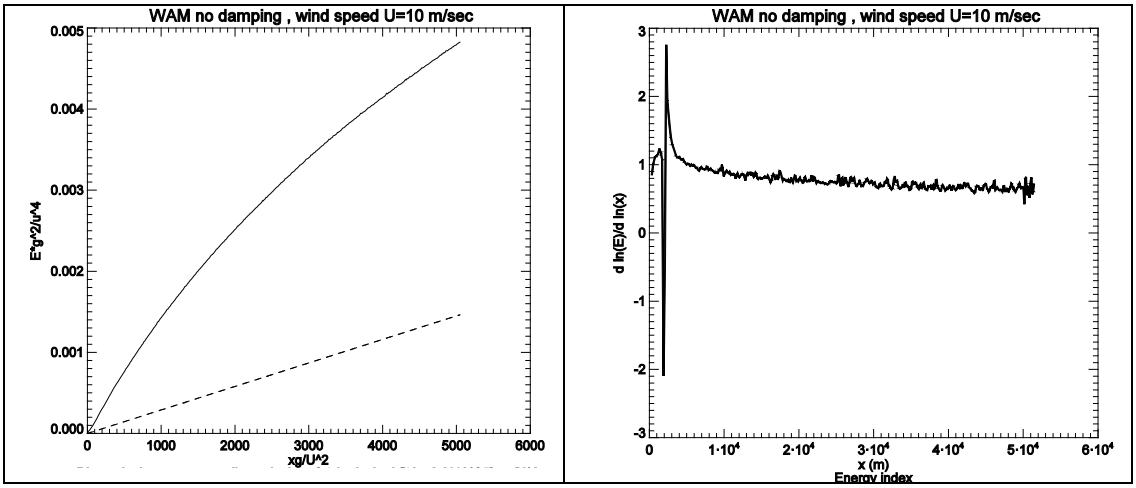

Fig.9 Same as Fig.1, but for Snyder S_{in}

Dependence of mean frequency against the fetch is shown on ***Fig.10*** is in not good correspondence with ***ZRP*** numerical results, and fairly good correspondence with self-similar solution index ***q=0.3***

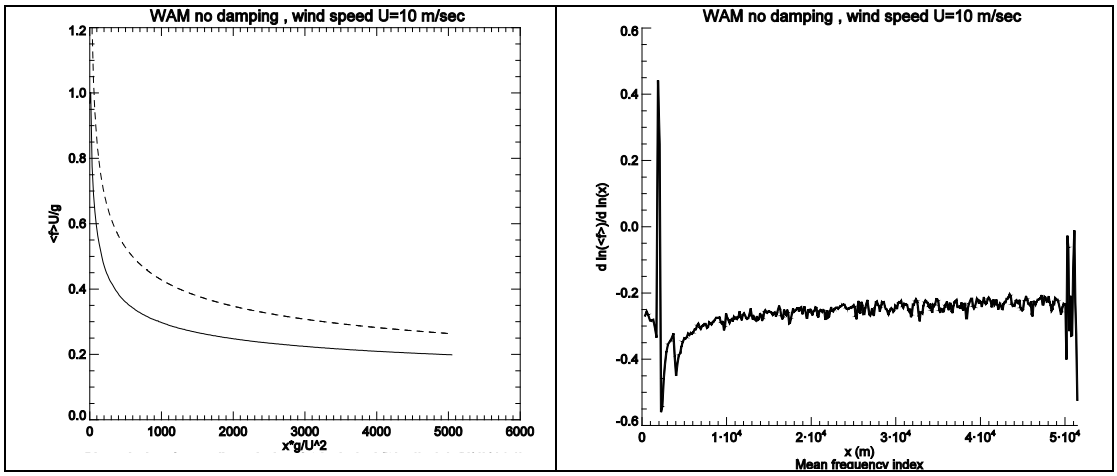

Fig.10 Same as Fig.2, but for Snyder S_{in}

Left-hand side of ***Fig.11*** presents directional spectrum as a function of frequency in logarithmic coordinates. One can easily see:

- the spectral maximum area
- Kolmogorov-Zakharov segment $\sim \omega^{-4}$
- Phillips high frequency tail $\sim \omega^{-5}$

Right side of ***Fig.11*** shows log-log derivative of the energy curve from ***Fig.9***, which corresponds to the exponent of the local power law. Again, one can see the areas corresponding Kolmogorov-Zakharov index ***-4*** and Phillips index ***-5***. The value of the index to the left side of ***-4*** has a tendency to grow, which qualitatively corresponds to the "inverse cascade" Kolmogorov-Zakharov index ***-11/3***.

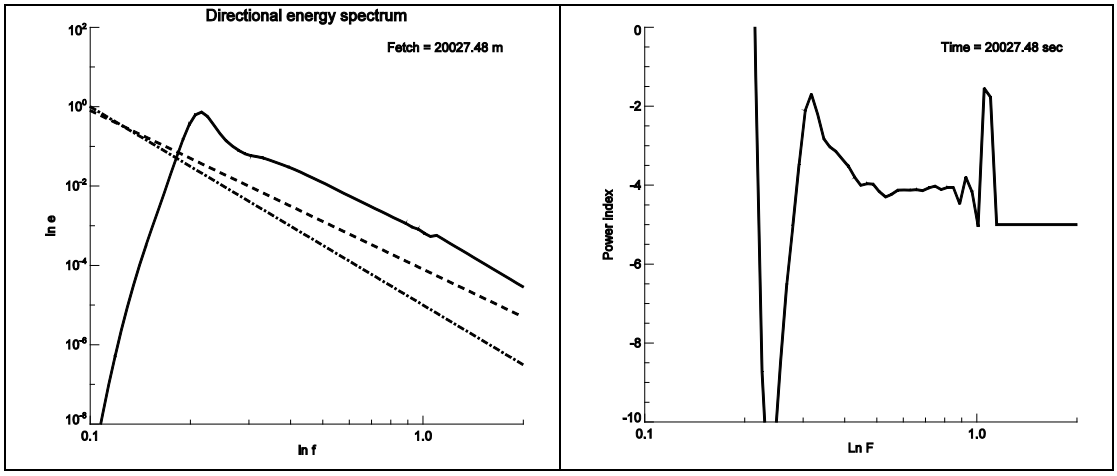

Fig.11 Same as Fig.3, but for Snyder S_{in}

Fig.12 presents the combination ***(10q-2p)*** as function of fetch. Again, it is in perfect accordance with the theoretical relation Eq.(4)! As in Chalikov case it means that despite incorrect values of ***p*** and ***q*** along the fetch, their combination ***(10q-2p)*** still holds in complete accordance with theoretical prediction, i.e. self-similarity is also fulfilled ***locally*** in Snyder case.

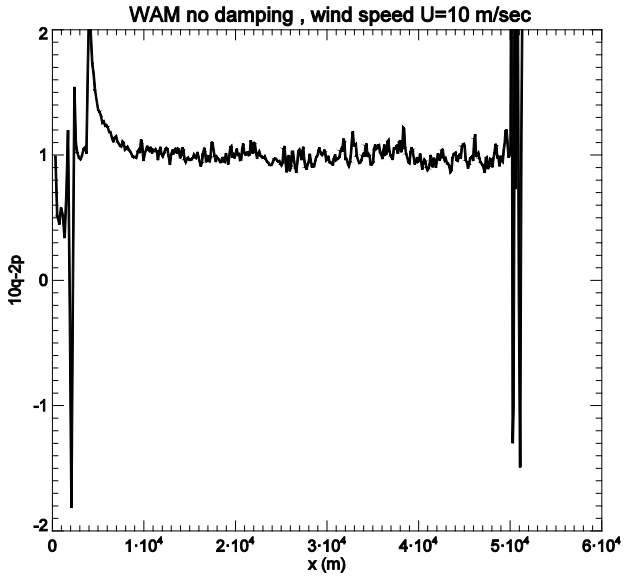

Fig.12 Same as Fig.4, but for Snyder S_{in}

Test of WAM3 form of S_{in}

Fig.13 shows that total energy growth along the fetch dramatically underestimates ***ZRP*** simulation, and has the value of growth exponent ***p*** asymptotically going to ***0*** versus fetch coordinate ***x***.

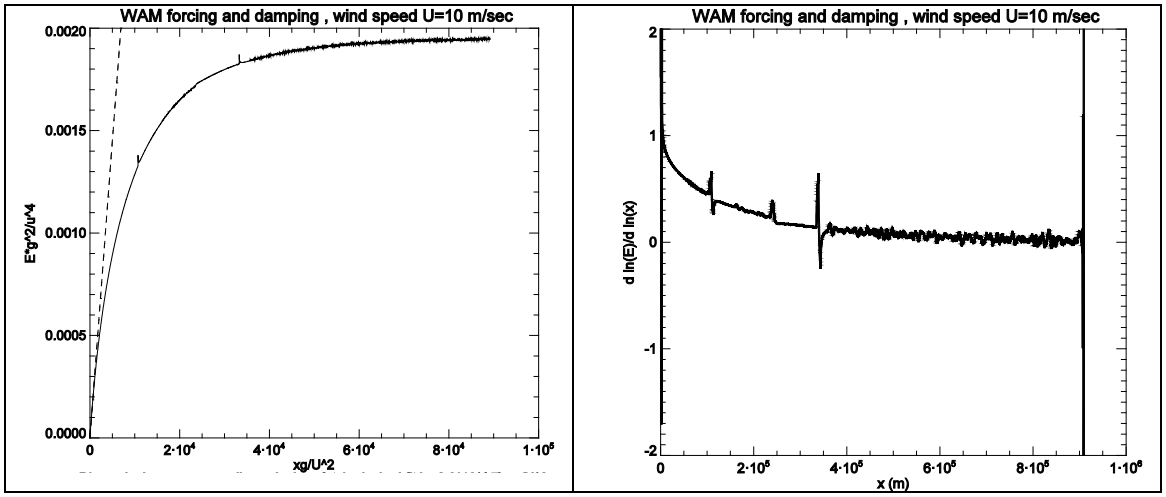

Fig.13 Same as Fig.1, but for WAM3 S_{in}

Dependence of the mean frequency against the fetch shown on ***Fig.14*** demonstrates strong discrepancy with ***ZRP*** results and corresponding self-similar solution index ***q*** also goes to ***0***:

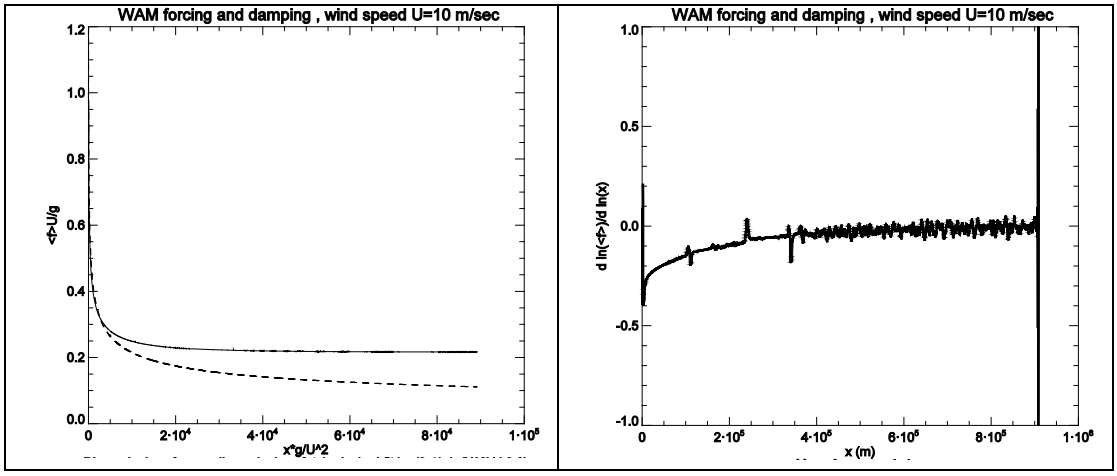

Fig.14 Same as Fig.2, but for WAM3 S_{in}

Left side of ***Fig.15*** presents directional spectrum as a function of frequency in logarithmic coordinates. One can see:

- the spectral maximum area
- Kolmogorov-Zakharov segment $\sim \omega^{-4}$
- Phillips high frequency tail $\sim \omega^{-5}$

Right side of ***Fig.15*** shows log-log derivative of the energy curve from ***Fig.13***, which corresponds to the exponent of the local power law. Again, one can see the areas corresponding Kolmogorov-Zakharov index ***-4*** and Phillips index ***-5***. The value of the index to the left side off ***-4*** has the tendency to grow, which qualitatively corresponds to the "inverse cascade" Kolmogorov-Zakharov index ***-11/3***.

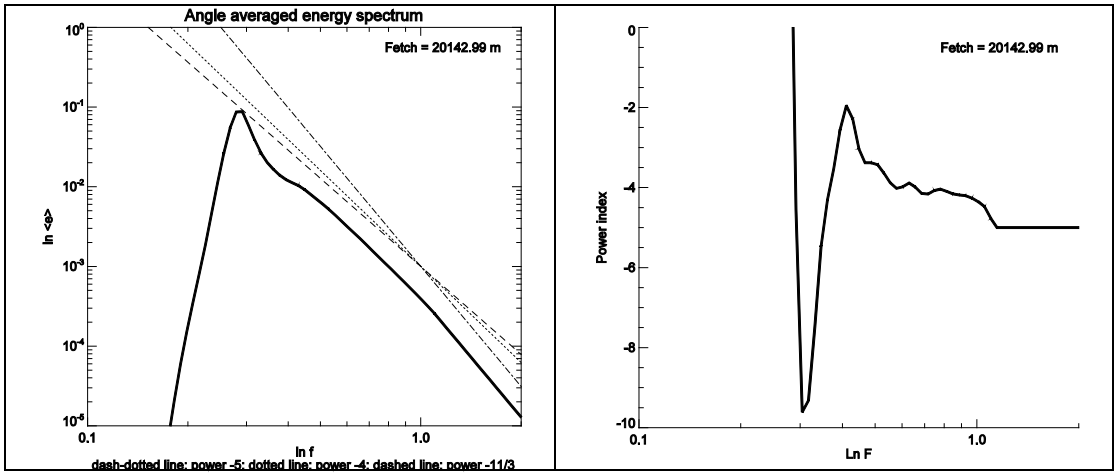

Fig.15 Same as Fig.3, but for WAM3 S_{in}

Fig.16 presents combination ***(10q-2p)*** as function of the fetch coordinate ***x***. It is in total disagreement with the theoretical predictions. There is no any indication of even local fulfillment of the "magic relation" Eq.(4).

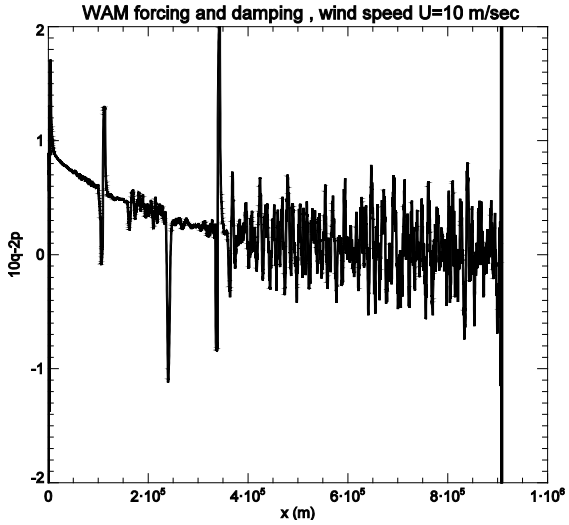

Fig.16 Same as Fig.4, but for WAM3 S_{in}

Summary of testing for different wind input terms

We applied set of nonlinear tests to different kinds of wind input terms and there are several conclusions we can make:

1. ***ZRP*** forcing term perfectly satisfies theoretical criteria like Kolmogorov-Zakharov spectrum $\sim \omega^{-4}$, self-similar solutions with exponents ***p=1*** and ***q=3***, "magic relation" ***10p-2q=1*** and more than a dozen of real experiments, see Eqs.(3)-(7) and ***Table 1***. Therefore, it can serve as a benchmark.
2. All wind input terms pass the test for presence of Kolmogorov-Zakharov law $\sim \omega^{-4}$
3. ***WAM3*** case fails to pass all the tests except test #2
4. ***Chalikov*** case fails ***p*** and ***q*** test, but passes "magic relation" test (quazi-self-similarity)
5. ***Snyder*** case "approximately" passes ***p-*** and ***q***-test and the "magic relation" one.

In a nutshell, the nonlinearity influence is so strong in the dynamics of HE that one can't "spoil" Kolmogorov-Zakharov law $\sim \omega^{-4}$ for any tested wind input term S_{in}. Self-similarity tests like ***p-*** and ***q-*** tests are more sophisticated one. And "magic relation" test is probably somewhere in-between versus detection of the "quality" of particular wind input term.

2. Universality of wind-wave growth

Nowadays, studies of wind-driven sea waves are usually focused on wind forcing rather than on the effect of inherent nonlinear wave dynamics. We propose a simple relationship between instant wave steepness and time or fetch of wave development expressed in wave periods or lengths

$$\mu^4 \nu = \alpha_0^3 \tag{9}$$

Here $\mu = E^{1/2}\omega_p^2 / g$ is wave steepness defined in terms of total wave energy E and spectral peak frequency ω_p, ν is a number of waves. For the duration-limited setup one has

$$\nu = \omega_p t \tag{10}$$

For the fetch-limited case we keep

$$\nu = 2k_p x \tag{11}$$

where coefficient 2 reflects the ratio of phase and group velocity of deep water waves. With Eqs. (10), (11) the universal constant α_0 has to take different values for duration- and fetch-limited setups. We introduce two different constants $\alpha_{0(d)} = 0.7$ and $\alpha_{0(f)} = 0.62$ based on our previous numerical and experimental studies **[R29]**, **[R32]**.

The law Eq. (9) does not contain wind-sea interaction parameters explicitly and relies upon asymptotic theory where wave nonlinearity is assumed to be a leading physical mechanism. The validity of this law is illustrated by results of numerical simulations of growing wind seas.

Numerical studies of wave growth for duration-limited setup

Fig.17 shows the results of simulations of duration-limited growth within the HE with the exact calculation of nonlinear term. The strong tendency of the invariant Eq. (9) to attract the theoretical limit $\alpha_{0\{d\}} = 0.7$ is seen fairly well.

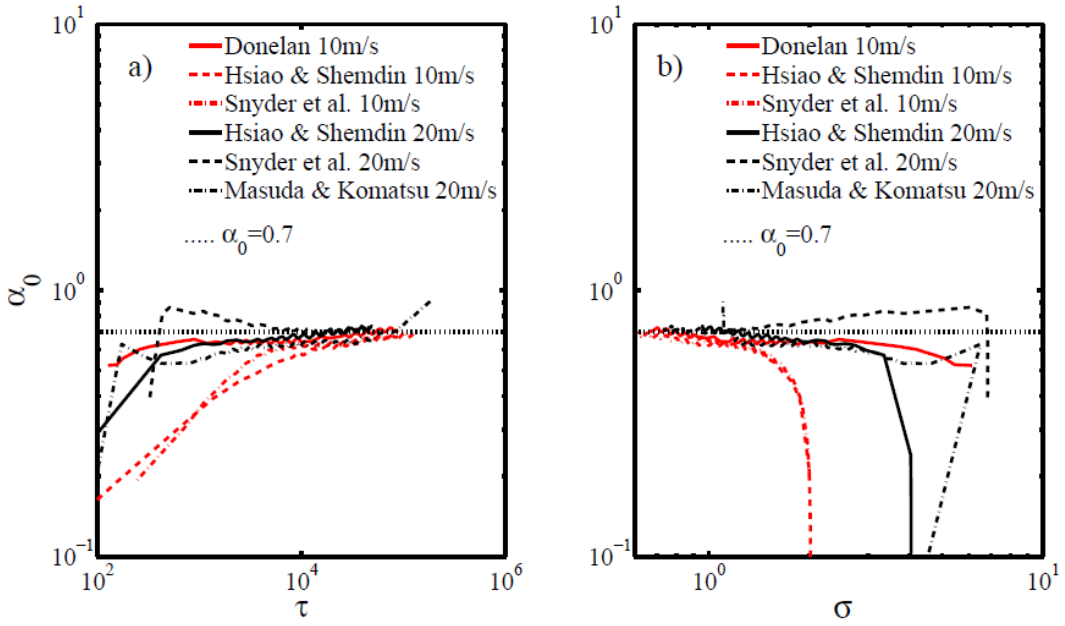

Fig.17 Dependence of parameter $\alpha_0 = (\mu^4 \nu)^{1/3}$***: (a) non-dimensional duration*** $\tau = gt/U_{10}$ ***and (b) inverse wave age*** $\sigma = \omega_p U_{10}/g$ ***in simulations of duration-limited wind wave growth [R29], [R30], [R31]. Simulation setups (wind input parameterization and wind speed) are given in legends. The horizontal dotted line shows theoretical value*** $\alpha_{0(d)} = 0.7$**.**

Numerical studies of wave growth for fetch-limited setup

This case has been considered in terms of dimensionless dependencies of wave height on wave period. Within the proposed approach that does not rely upon wind parameters and dimensionless variables can be introduced as follows for duration-

$$\tilde{H} = H/gt^2; \quad \tilde{T} = T/2\pi t \tag{12}$$

and fetch-limited setups

$$\tilde{H} = H/x; \quad \tilde{T} = T\sqrt{g/8\pi^2 x} \tag{13}$$

Simulations of the fetch-limited growth have been carried out by A. Pushkarev (Zakharov, Pushkarev 2012) and used considered evolution of wave spectra both in time and space. ***Fig.18*** shows an

intermediate nature of asymptotic of the solutions. In the left panel the scaling Eq.(13) has been used. The fetch-limited asymptotical dependence

$$\widetilde{H} = 5.59\widetilde{T}^{5/2}$$

works quite well in a range. For large time the corresponding curves are tending to a saturation: wave field start to develop in a duration-limited regime.

The right panel of ***Fig.18*** shows the same results in terms of time scaling Eq. (12) that gives the law

$$\widetilde{H} = 3.06\widetilde{T}^{9/4}$$

Again, we see proximity of the simulation results to the theoretical curve in an intermediate range of dimensionless wave periods.

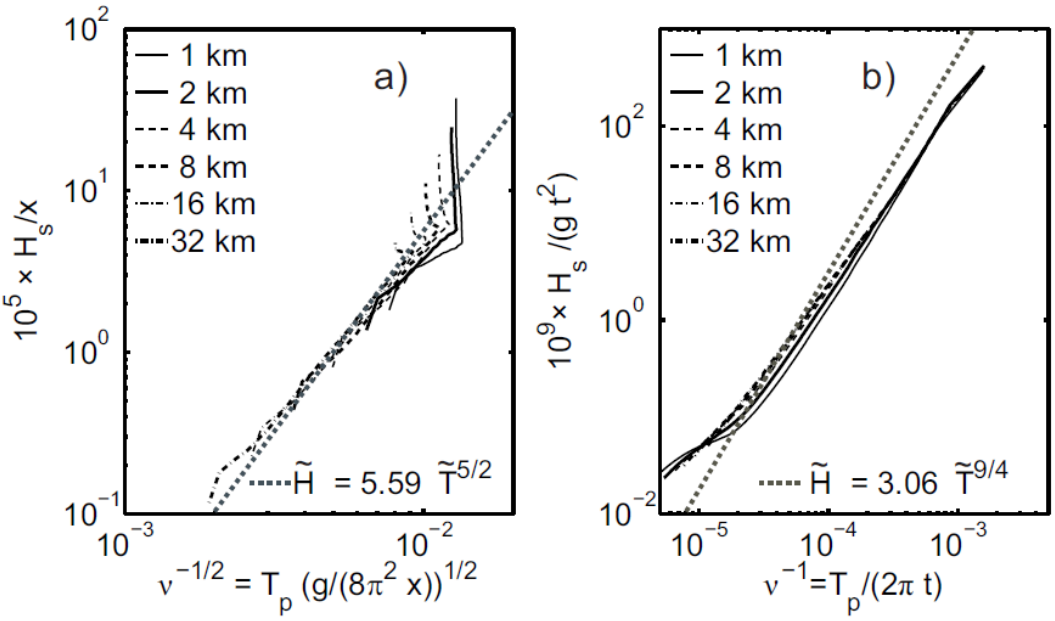

Fig.18 Wave growth curves in simulations of fetch-limited setup (Zakharov, Pushkarev 2012) within: (a) fetch scaling; (b) duration scaling. Curves are given for fixed fetches 1, 2, 4, 8, 16, 32 km (see legends). Theoretical dependencies are shown by dotted lines.

Thus, the proposed theoretical law Eq.(9) is verified in an extensive numerical study and provides the tool for diagnosis of wind wave growth.

3. Comparison of compact equation for surface waves with fully nonlinear equations

We compare applicability of the recently derived compact equation for surface waves with the fully nonlinear equations. Strongly nonlinear phenomena, namely modulational instability and breathers with the steepness $\mu \approx 0.4$ are compared in numerical simulations using both models.

For the fully nonlinear model we have chosen free surface equation written in the conformal variables, $R-V$ -equations **[R36]** :

$$R_t = i(UR_w - RU_w), V_t = i(UV_w - RB_w) + g(R-1) \tag{14}$$

Now U and B are the following:

$$U = \hat{P}(V\overline{R} + \overline{V}R)B = \hat{P}(V\overline{V})$$

So, these exact Eqs.(14) give us reference solutions to compare with.

For the approximate model we used compact equations derived in **[R37], [R38]** :

$$\begin{aligned} i\frac{\partial b}{\partial t} &= \hat{\omega}_k b + \frac{i}{4}\hat{P}^+\left[b^*\frac{\partial}{\partial x}(b'^2) - \frac{\partial}{\partial x}(b^{*\prime}\frac{\partial}{\partial x}b^2)\right] \\ &-\frac{1}{2}\hat{P}^+\left[b\cdot\hat{k}(|b'|^2) - \frac{\partial}{\partial x}(b'\hat{k}(|b|^2))\right] \end{aligned} \tag{15}$$

Transformation from $b(x,t)$ to physical variables $\eta(x,t)$ and $\psi(x,t)$ can be recovered from canonical transformation. Here we write this trasformation up to the second order:

$$\eta(x) = \frac{1}{\sqrt{2}g^{\frac{1}{4}}}(\hat{k}^{\frac{1}{4}}b(x) + \hat{k}^{\frac{1}{4}}b(x)^*) + \frac{\hat{k}}{4\sqrt{g}}[\hat{k}^{\frac{1}{4}}b(x) - \hat{k}^{\frac{1}{4}}b^*(x)]^2, \psi(x) =$$

$$-i\frac{g^{\frac{1}{4}}}{\sqrt{2}}(\hat{k}^{-\frac{1}{4}}b(x) - \hat{k}^{-\frac{1}{4}}b(x)^*) + \frac{i}{2}[\hat{k}^{\frac{1}{4}}b^*(x)\hat{k}^{\frac{3}{4}}b^*(x) - \hat{k}^{\frac{1}{4}}b(x)\hat{k}^{\frac{3}{4}}b(x)]$$

$$+\frac{1}{2}\hat{H}[\hat{k}^{\frac{1}{4}}b(x)\hat{k}^{\frac{3}{4}}b^*(x) + \hat{k}^{\frac{1}{4}}b^*(x)\hat{k}^{\frac{3}{4}}b(x)].$$

Here $\hat{H}$ - is Hilbert transformation with eigenvalue $isign(k)$.

Modulational instability of wave train

We performed numerical simulation of the modulational instability of the homogeneous wavetrain in the framework of compact Eq.(15). Initial steepness of the wave train was equal to $\mu = 0.095$. This value was chosen for comparison with the earlier simulation in the framework of fully nonlinear simulation **[R39], [R40].** One can see in ***Fig.19*** and ***Fig.20*** that both waves coincide in details. Different time of their appearance is due to slightly different values of perturbations.

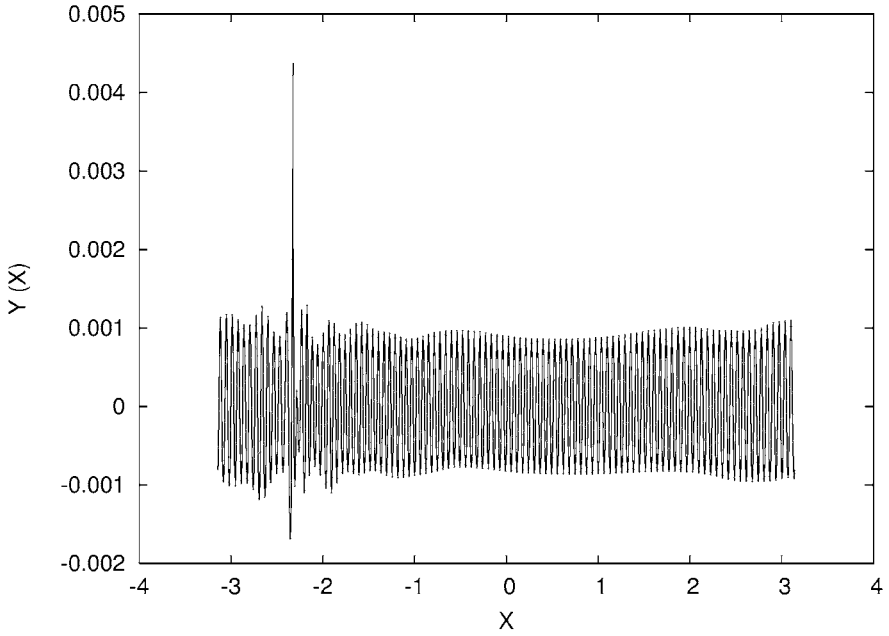

Fig.19 Freak-wave formation after t=802 (fully nonlinear equation)

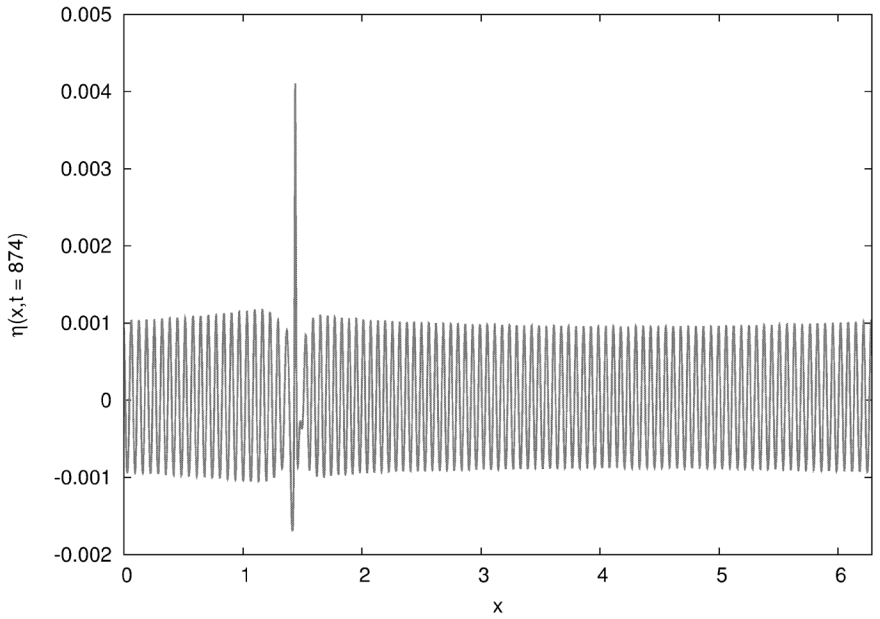

Fig.20 Freak-wave formation after t=874 (compact equation)

Breathers

We have also performed simulations of narrow breathers both in the framework of fully nonlinear conformal Eq.(14) and compact Eq.(15). Here we present pictures of the steepness of the surface of the fluid:

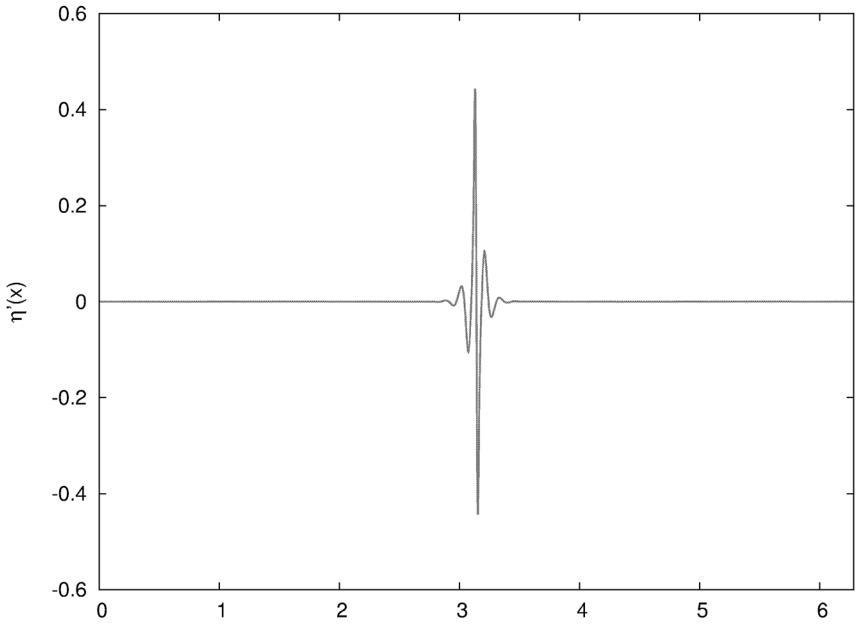

Fig.21 Steepness of the breather (compact equation).

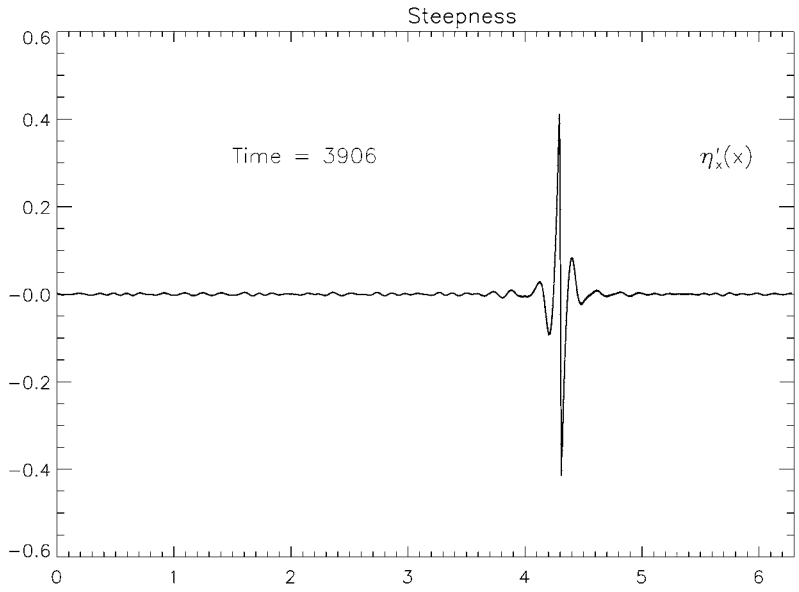

Fig.22 Profile of steepness (fully nonlinear equations).

We have demonstrated that compact equation, although approximate, quantitatively describes strongly nonlinear phenomena at the surface of potential fluid. We also have studied especially nonlinear stage of modulational instability up to the freak-wave formation and propagation of very steep breather.

3. Modulational instability and coherent event for surface waves. Air-surface interaction.

The research has dealt mainly with different aspects of nonlinear waves relevant to understanding of ocean wave dynamics. It is well known that shallow water is stable in particular at $kh<1.36$ where k is the wave number and h is the water depth -- modulational instability cannot take place in these conditions. However, it has been shown in **[P3]** that two waves propagating in shallow water at different angles can be unstable to long wave modulations. Analytical solutions of the coupled nonlinear Schrödinger equation are reported and discussed in **[P3].** This family of solutions includes bright-dark and dark-dark rogue waves. The link between modulational instability (MI) and rogue waves is displayed by showing that only a peculiar kind of MI, namely baseband MI, can sustain rogue-wave formation. The existence of vector rogue waves in the defocusing regime is expected to be a crucial progress in explaining extreme waves in a variety of physical scenarios described by multi-component systems, from oceanography to optics and plasma physics.

Coherent structures in shallow water are studied in paper **[P4]**. Within a number of approximations, the dynamics of surface gravity water waves in finite depth can be described by self-defocusing nonlinear Schrodinger equation. It is well known that dark solitons are exact solutions of such equation. In the present paper it has been shown that gray solitons can be produced in the wave tank experiments.

Air-water interaction phenomena taking place during the breaking of ocean waves are investigated in **[P5]**. The study is carried out by exploiting the combination between potential flow method, which is used to describe the evolution of the wave system up to the onset of the modulational instability, and two-fluid Navier–Stokes solver which describes strongly non-linear air–water interaction taking place during breaking events. The potential flow method is based on fully non-linear mixed Eulerian–Lagrangian approach, whereas the two-fluid model uses a level-set method for the interface capturing. The method is applied to study the evolution of a modulated wave train composed by a fundamental wave component with two side band disturbances. It is shown that breaking occurs when the initial steepness exceed threshold value. Typical wave breaking events are shown on ***Fig.23***. Once the breaking starts, it is not just a single event, but it is recurrent with a period associated to the group velocity. Results are presented in terms of free surface shapes, velocity and vorticity fields, energy and viscous dissipation. The analysis reveals the formation of large vortex structures in the air domain, which are originated by the separation of the air flow at the crest of the breaking wave. This forms drag associated with the flow separation process and significantly contributes to the dissipation of the energy content of the wave system.

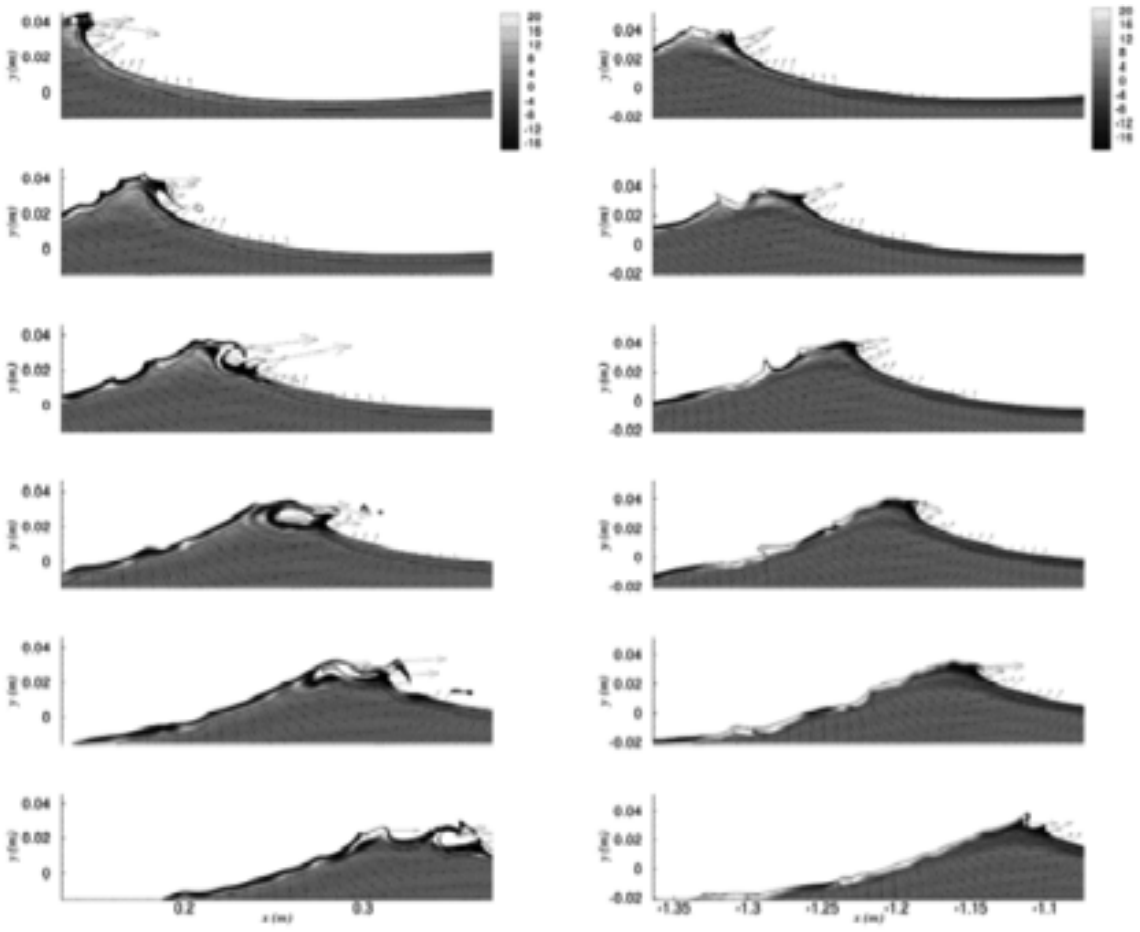

Fig.23 Surface elevation during wave breaking from numerical computation of the Navier Stokes equation.

Paper **[P6]** is an interdisciplinary paper where some properties of the nonlinear energy transfer are observed in numerical computations of Nonlinear Schrodinger equation, and in the optical fibers experiments. In particular it has been shown that the phenomenon of intermittency takes place also in integrable systems. This is a very important result that can be used to understand statistical properties of small scales ocean waves.

IMPACT/APPLICATIONS

- Improvement of the quality of operational wave forecasting programs.
- Better understanding the nonlinear ocean surface wave dynamics
- Creation of simplified models of nonlinear surface waves
- Better understanding of ocean waves – airflow interaction

RELATED PROJECTS

NONE

REFERENCES

[R1] S.I.Badulin, A.N.Pushkarev, D.Resio, and V.E.Zakharov, Self-similarity of wind-driven sea, Nononlinear Processes in Geophysics, 12, 891-945, 2005

[R2] I. R.Young, Wind Generated Ocean Waves, Elsevier 1999

[R3] Tsagareli, A.Babanin, D. Walker and I. Young, Numerical Investigation of Spectral evolution of Wind Waves. Part I: Wind-Input Source Function, JPO, 40, 656-666, 2009

[R4] I.R.Young, A.V. Babanin, Spectral Distribution of Energy Dissipation due to Dominant Wave Breaking, JPO, 36, 376-394

[R5] Tolman, H. L., D. Chalikov, Source terms in a third-generation wind-wave model, J. Phys. Oceanogr., **26**, 2497-251, 1996

[R6] Janssen P. A. E. M., Quasilinear approximation for the spectrum of wind-generated water waves, J. Fluid Mech., 117, 493-506, 1982

[R7] S. E. Belcher, J. C. R. Hunt, Turbulent flow over hills and waves, Annual Review of Fluid Mechanics, 30, 507-538, 1998

[R8] J.W.Miles, On the generation of surface waves by shear flows, J.FluidMech, 3, 185-204, 1957

[R9] Yu.Troitskaya, D. Sergeev, O. Ermakova and G. Balandina, Statistical parameters of the Air Boundary Layer over Steep Water Waves Measured by PIV Technique, Journal of Physical Oceanography, 41, 1421-1454, 2011

[R10] Snyder, R.L., F.W. Dobson, J.A. Elliott, and R.B. Long, Array measurements of atmospheric pressure fluctuations above surface gravity waves. *J. Fluid Mech.*, 102, 1-59, 1981

[R11] M. Donelan, A. Babanin, I.R.Young and M. Banner, Waves-follower field measurements of the wind-input spectral function. Part II: Parameterization of the Wind Input, JPO, 36, 1672-1689, 2006

[R12] V. E. Zakharov, On the energy balances in wind-driven sea *Phys.Scr., 142,* 2010

[R13] V.E. Zakharov, S.I.Badulin, On energy balance in wind-driven sea, Doklady Akademii Nauk, vol.440, N5, pp.691-695, 2011

[R14] K.Hasselmann, D.B.Ross, P.Muller and E.Sell, A parametric wave prediction model, Journal of Physical Ocenography, vol.6, 200-228, 1976

[R15] Plant W.J., A relationship between wind stress and wave slope, Journal geophysical research, 87 (C5), 1961-67

[R16] Cavaleri et al. (The WISE GroupWave modeling – The state of the art, Progr. Oceanogr., doi:10.1016/j.pocean.2007.05.005, 72p, 2007

[R17] A. Pushkarev, D. Resio, V. Zakharov, Weak turbulent approach to the wind-generated gravity sea waves, Physica D 184 (1-4) 29-63 (2003): in "Complexity and Nonlinearity in Physical Systems" — a special issue to honor A. Newell

[R18] S.I. Badulin, A.N. Pushkarev, D.Resio, V.E.Zakharov, Self-similarity of wind-driven seas, Nonlin. Process Geophys, 12 (6), 891-945 (2005)

[R19] V. E. Zakharov, D. Resio, A. Pushkarev, New wind input term consistent with experimental, theoretical and numerical considerations, arXiv:1212.1069 [physics.ao-ph]

[R20] Resio D., Long C., Equilibrium-range constant in wind-generated spectra, Journal of Geophysical Research, v.109, CO1018, 2004

[R21] Long, C.E, and D. Resio, Wind wave spectral observations in Currituck Sound, North Carolina Journal of Geophysical Research, v. 112, CO5001, 2007

[P23] A.Pushkarev, V.E.Zakharov, Quasibreathers in the MMT model, Physica D, 248, 55-61, 2013

[R24] Paul Huang, Yakov Toporkov, Mark Sitten and Steven Menk, Measuring wave breaking by radar, Presentation on WISE 2013 meeting, College Park, MD, USA

[R25] Paul Huang, Yakov Toporkov, Mark Sitten and Steven Menk, Mapping surface currents and waves with Interoferomic Synthetic Aperture Radar in coastal waters: Observation of wave Breaking in Swell-Dominant Conditions, JPO, pp 563-581, 2013

[R26] D. Chalikov, The Parameterization of the Wave Boundary Layer. J. Phys. Oceanogr., 25, 1333–1349, 1995

[R27] Snyder R.L., Dobson F.W., Elliott J.A. and Long R.B., Array measurement of atmospheric pressure fluctuations above surface gravity waves, J. Fluid Mech., 102, 1-59, 1981

[R28] User manual and system documentation of WAVEWATCH III, Hendrik L. Tolman, Environmental Modeling Center, Marine Modeling and Analysis Branch, 2013

[R29] Badulin, S. I., Babanin, A. V., Resio, D. & Zakharov, V. Weakly turbulent laws of wind-wave growth. *J. Fluid Mech.* 591, 339–378, 2007

[R30] Badulin, S. I., Babanin, A. V., Resio, D., Zakharov V., Numerical verification of weakly turbulent law of wind wave growth. In *IUTAM Symposium on Hamiltonian Dynamics, Vortex Structures, Turbulence. Proceedings of the IUTAM Symposium held in Moscow, 25-30 August, 2006* (ed. A. V. Borisov, V. V. Kozlov, I. S. Mamaev & M. A. Sokolovskiy), *IUTAM Bookseries*, vol. 6, pp. 175–190. Springer, ISBN: 978-1-4020-6743-3, 2008

[R31] Badulin, S. I., Pushkarev, A. N., Resio, D., Zakharov V. E., Self-similarity of wind-driven seas. *Nonl. Proc. Geophys.* 12, 891–946, 2005

[R32] Gagnaire-Renou E., Benoit, M., Badulin, S.I., On weakly turbulent scaling of wind sea in simulations of fetch-limited growth. *J. Fluid Mech.* 669, 178–213, 2011

[R33] Pushkarev, A. N., Resio, D., Zakharov V. E., Weak turbulent theory of the wind-generated gravity sea waves. *Phys. D: Nonlin. Phenom.* 184, 29–63, 2003

[R34] Zakharov, V. E., Theoretical interpretation of fetch limited wind-driven sea observations. *Nonl. Proc. Geophys.* 12, 1011–1020, 2005

[R35] Zakharov, V. E., Energy balance in a wind-driven sea. *Phys. Scr.* T142, 014052, 2010

[R36] Dyachenko, A.I.: On the dynamics of an ideal fluid with a free surface. Doklady Mathematics, **63(1)**, 115—118, 2001

[R37] Dyachenko, A.I. and Zakharov, V.E.: Compact equation for gravity waves on deep water, JETP Letters, **93(12)**, 701—705, 2011

[R38] Dyachenko, A.I., Zakharov, V.E.: A dynamic equation for water waves in one horizontal dimension. Europ. J. Mech. B **32**, 17—21, 2012

[**R39]** Dyachenko, A.I. and Zakharov, V.E.: Modulation Instability of Stokes Wave → Freak Wave, JETP Letters, 81(6), 255—259, 2005

[R40] Zakharov, V.E., Dyachenko, A.I. and Prokofiev, A.O.: Freak waves as nonlinear stage of Stokes wave modulation instability, European Journal of Mechanics B/Fluids, v. **120(5)**, 677 – 692, 2006

PUBLICATIONS

[P1] Dyachenko A.I., Kachulin D.I. and Zakharov V.E., Freak waves at the surface of deep water, Journal of Physics: Conference Series, **510**, 012050, 2014 [published]

[P2] Dyachenko A.I., Kachulin D.I., and Zakharov V.E., Freak-waves: Compact Equation vs Fully Nonlinear One. in the book "Extreme Ocean Waves", Springer, E.Pelinovsky and C. Harif (Eds), [submitted]

[P3] Baronio, F., Conforti, M., Degasperis, A., Lombardo, S., Onorato, M., & Wabnitz, S., 2014 Vector Rogue Waves and Baseband Modulation Instability in the Defocusing Regime. *Physical Review Letters* 113, 034101, 2014 [published]

[P4] Chabchoub, A., Kimmoun, O., Branger, H., Kharif, C., Hoffmann, N., Onorato, M., Akhmediev, N., Gray solitons on the surface of water. *Physical Review E*, *89*(1), 011002, 2014 [published]

[P5] Iafrati, A., Babanin, A., & Onorato, M. Modeling of ocean–atmosphere interaction phenomena during the breaking of modulated wave trains. *Journal of Computational Physics*, *271*, 151-171, 2014 [published]

[P6] Randoux, S., Walczak, P., Onorato, M., & Suret, P. Intermittency in integrable turbulence, *Physical Review Letters*, *113*(11), 113902, 2014 [published]